FREEZE CASTING OF $Pb(Zr_xTi_{1-x})O_3$ WITH PSEUDOMONAS SYRINGAE

BY

SAMUEL LAMPHIER

A THESIS
SUBMITTED TO THE FACULTY OF

ALFRED UNIVERSITY

IN PARTIAL FULFILLMENT OF THE REQUIREMENTS
FOR THE DEGREE OF

MASTER OF SCIENCE

IN

MATERIALS SCIENCE AND ENGINEERING

ALFRED, NEW YORK

February, 2014

FREEZE CASTING OF $Pb(Zr_xTi_{1-x})O_3$ WITH PSEUDOMONAS SYRINGAE

BY

SAMUEL LAMPHIER

B.S. ALFRED UNIVERSITY (2011)

SIGNATURE OF AUTHOR (Signature on File)

APPROVED BY (Signature on File)

STEVEN PILGRIM, ADVISOR

(Signature on File)

WALTER SCHULZE, ADVISORY COMMITTEE

(Signature on File)

WILLIAM CARLSON, ADVISORY COMMITTEE

(Signature on File)

CHAIR, ORAL THESIS DEFENSE

ACCEPTED BY (Signature on File)

DOREEN D. EDWARDS, DEAN
KAZUO INAMORI SCHOOL OF ENGINEERING

ACKNOWLEDGMENTS

Steven Pilgrim

Walter Schulze

William Carlson

James Weigner

Swavek Zdzieszynski

Gerald Wynick

Steven Arrasmith

Alastair N. Cormack

John D'Angelo

Tyler Gubb

Ryan Dempsey

Danica Ostrander

Bu Wang

Larissa Buttaro

Erika Raye

To my friends that are not listed, you know who you are.

TABLE OF CONTENTS

LIST OF TABLES

LIST OF FIGURES

ABSTRACT

Centrifugal bio-freeze casting, (CBFC), is a revolutionary new technique for the production of near net shape piezoelectric components. CBFC exploits the unique ability of *Pseudomonas syringae* bacteria to promote ice formation near 0°C. By combining water, bacteria and $Pb(Zr_xTi_{1-x})O_3$ in a centrifuge, it is possible to produce dense near net shape green bodies which later undergo vacuum-assisted dehydration and sintering. CBFC is an environmentally favorable process which avoids the use of binders to make complex piezoelectric components for a variety of applications. The economic viability and simplicity of CBFC makes it attractive on an industrial level.

Introduction

This research seeks to produce higher quality compacts with improved green densities by incorporating bacteria into ceramic processes. Near net shape forming of ceramic bodies has received considerable attention with the increased need for complex ceramic parts[1]. A multitude of techniques and variations have been developed for near net shape formation. These techniques have common factors such as molds with minimal sintering shrinkage and the use of binders. High quality compacts require avoiding density gradients. Eliminating density gradients decreases warping during sintering. It is also necessary to avoid high solids loading which causes undesirable warping and cracking after solvent removal[2]. A well-dispersed suspension is critical for uniform sintering behavior while a poorly-dispersed system yields porosity or density gradients. Predictable shrinkage, minimal density gradients and avoidance of high solids loading are the primary requirements for producing high quality compacts. There are three main techniques used for near net shape production; "injection molding, gel casting, and freeze forming techniques[2]." This research implements Centrifugal bio-freeze casting as an environmentally friendly and economical method for the formation of near net shape piezoelectric ceramics.

Centrifugal freeze casting is a modern technique for the processing of dense ceramic bodies used in the ceramics industry. This process involves the preparation of a suspension which is simultaneously cooled and centrifuged. The process yields a near net shape piece which is later freeze-dried and sintered to achieve further densification[2]. Dense final products exhibit exceptional general properties. Near net shape forming is a minimal waste process that requires little machining. Freeze cast pieces exhibit excellent dimensional tolerance, where the precise shrinkage is known. Precise shrinkage is optimal for producing minimal waste and allows for the production of complex parts.

In the early 1970s two independent research groups (one in plant pathology and one in atmospheric science) discovered that *Pseudomonas syringae* possesses strong ice nucleation activity (INA)[3] promoting ice formation near 0°C. The performance of this bacteria is superior to even the best inorganic nucleating agent, AgI[4]. Deemed

"biological ice nucleators," *Pseudomonas syringae* serves environmentally as a cloud condensation nuclei. When water is cooled below its freezing point, it undergoes a phase change from a triple point at 0°C to a stable solid state. Centrifuging bacteria, water and ceramic powders leads to a process called centrifugal bio-freeze casting (CBFC) amenable to processing of dense, near net shape green bodies. CBFC eliminates binders making it a step closer to green processing. CBFC decreases chemical toxicity by removing the binder burnout phase completely.

CBFC relies on the use of ice nucleating bacteria and water to replace binders. The primary choice of bacteria is *Pseudomonas syringae.* This bacteria has had evolutionary history to optimize its interaction with water. It thrives on fruits and their nutrients by puncturing the skin of the fruit when temperatures in the surrounding environment approach 0°C. There are two types of *Pseudomonas syringae,* ice nucleation active (INA), and ice minus bacteria (IMB). IMB is recombinant DNA engineered to lack surface protein. INA bacteria uses proteins secreted through the pilus as ice nucleating templates in order to organize water molecules. The protein organized water molecules are thermodynamically preferred ice templating sites, called an ice embryo. The templating sites are the framework for ice production.

This work applies centrifugal freeze casting with the addition of *Pseudomonas syringae* in order to process lead zirconate titanate ceramics. Lead zirconate titanates are the primary commercial piezoelectric ceramics. Common uses of $Pb(Zr_xTi_{1-x})O_3$ include naval sonar, ultrasonics, medical devices and spark lighters. By providing a low-cost method of forming, such as CBFC of $Pb(Zr_xTi_{1-x})O_3$ ceramics, additional applications may become possible.

Scope

The objective of this thesis is to examine the viability of the biologically enhanced centrifugal freeze casting system for the production of dense, low-cost, $Pb(Zr_xTi_{1-x})O_3$ prototype components. Using an environmental scanning electron microscope, (ESEM) and X-ray diffraction (XRD) it is possible to investigate *Pseudomonas syringae* and to understand the impact of cell wall proteins and their effect on the freezing temperature of water. By studying centrifuge forming techniques and the freezing properties of *Pseudomonas syringae* it may be possible to prepare dense green body $Pb(Zr_xTi_{1-x})O_3$.

This work exploits the unique properties of water in combination with two common materials: Icemax™ and lead zirconate titanate powder. Icemax™ INA proteins are used to produce artificial snow. Icemax™ consists of *Pseudomonas syringae* coated in sodium sulfate decahydrate which acts as a dispersing agent.

In this thesis, studies have been conducted on the preparation and the drying of $Pb(Zr_xTi_{1-x})O_3$ suspensions incorporating *Pseudomonas syringae*. This type of unique process has heretofore not been studied and this research focuses on this method of preparation. A spray dried powder was provided by the Lockheed Martin Corporation[5] for the possible processing of $Pb(Zr_xTi_{1-x})O_3$ ceramic rings.

Background and Literature Review

The dominant hexagonal form of ice is less dense than water and therefore floats. By raising the temperature at which ice formation begins, the volumetric expansion may be decreased yielding a higher density body. Since *Pseudomonas syringae* possesses the highest ice nucleation temperature of all the known bacteria, it is hypothesized to act as an ideal candidate. This thesis combines water, *Pseudomonas syringae* and $Pb(Zr_xTi_{1-x})O_3$ ceramic powder in order to form dense green body ceramics. As a result of this research, new processing capabilities may also be developed by combining CBFC and $Pb(Zr_xTi_{1-x})O_3$.

A. Characteristics and behavior of water

"When water changes phase from liquid to vapor (evaporation) or from liquid to solid (freezing), energy is either gained or lost as heat flow[6]." Water, as a polar molecule with high surface tension and adhesion properties, may crystallize into 15 different types of ice. These phases are amorphous ice, Ice I, containing both hexagonal ice and cubic ice, and ice II through ice XV. Hexagonal ice is the predominate form of ice found on the Earth, although recent studies suggest the ice formation in cloud systems may be cubic. Amorphous ice can form in a range of pressures by hyperquenching water. Similar to a metallic glass it is thermodynamically metastable. Hexagonal crystalline ice is found on roads, buildings and in streams. A second metastable ice called "cubic ice" is also found to be naturally occurring[7].

At the equilibrium freezing point of 0°C water begins to freeze just below this temperature in the presence of nucleation sites (at standard temperature and pressure). However, in the absence of nucleation sites, deionized water must be cooled below -40°C to start homogenous nucleation[6]. The two most common forms are hexagonal (I_h) and cubic ice (I_c), Figure 1.

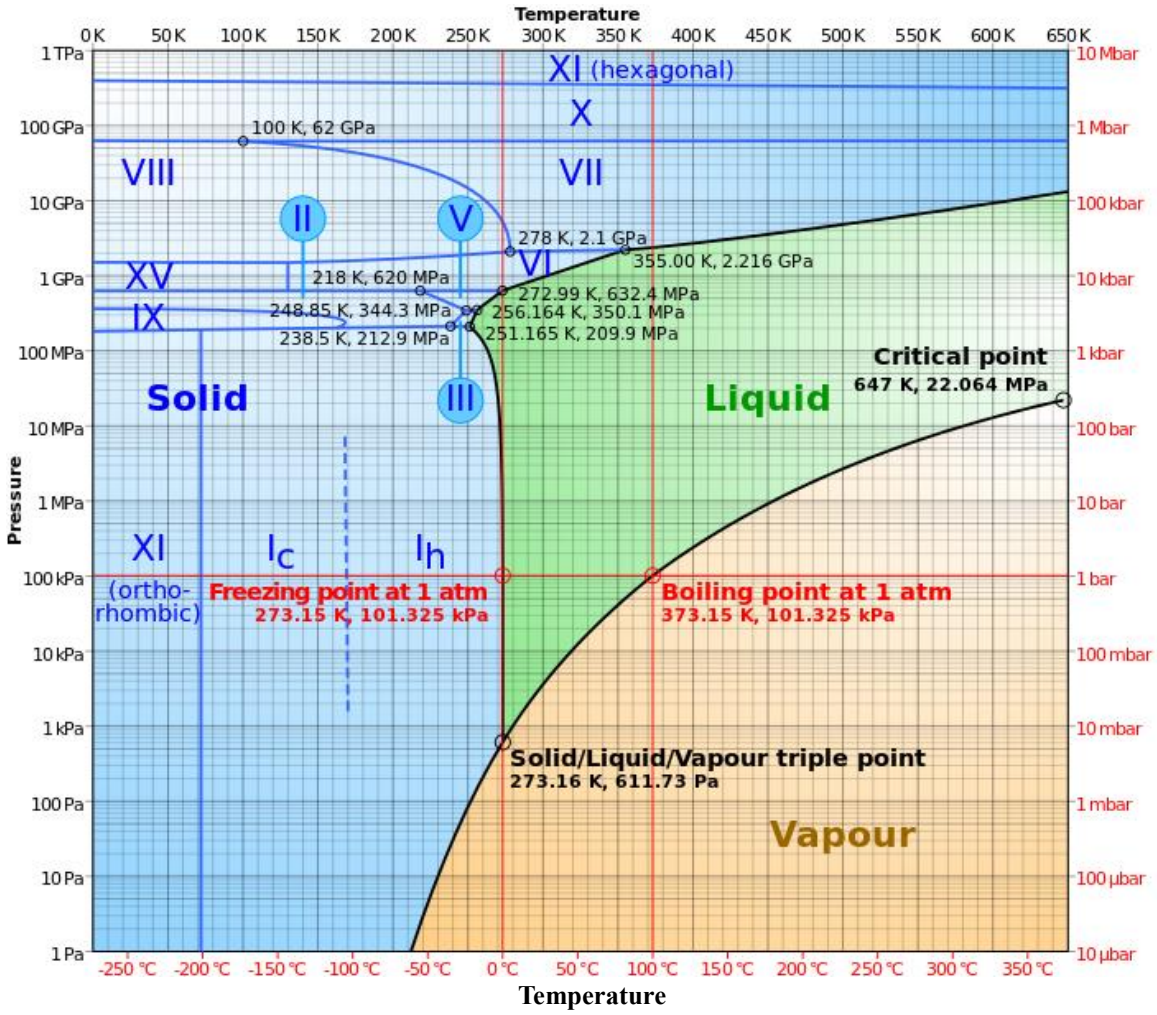

Figure 1: Phase diagram of water[8].

Although cubic ice is stable below -100°C (Figure 1), the reconstructive phase transformation requires substantial over-heating to change to hexagonal ice. Cubic ice exists up to -53.15°C at which point it transforms to hexagonal ice existing up to 0°C. Hexagonal or ordinary ice (I_h) corresponds to the hexagonal crystal structure[9]. The structures of hexagonal and cubic ice are shown in Figure 2.

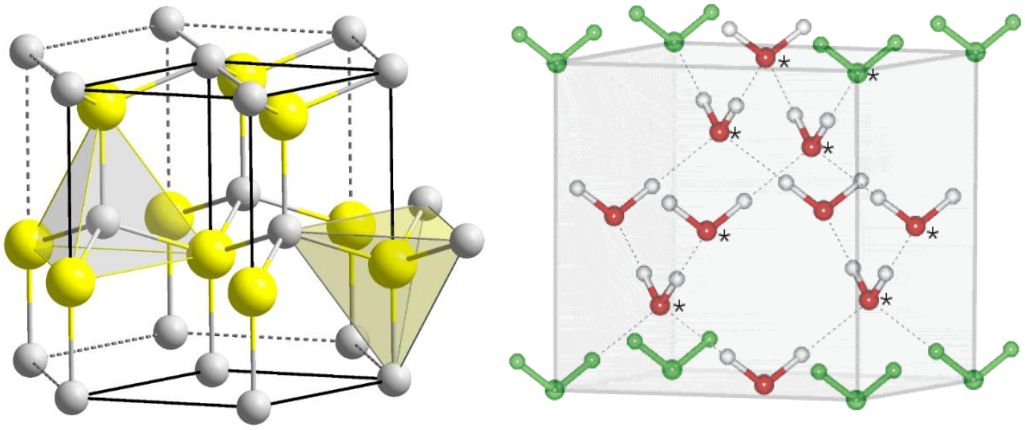

Figure 2: Hexagonal ice (left), cubic ice (right)[10].

Water is often studied with regard to biology where the growth of ice crystals can puncture cell walls and destroy cells. Slowly cooled samples with the lowest degree of supercooling produced the most damage as noted in several papers[11,12,13]. This indicates that a faster rate of cooling is more desirable for solidification processes. On the other hand, flash freezing causes rapid and substantial expansion in the bulk samples increasing the chance for cracks and other defects. Large crystal formations can also push particles with the ice front causing non-uniform ceramic bodies to develop. During non-centrifugal freeze casting, this is generally perceived as a negative side effect. However, during CBFC, the ice front consistently pushes upward against the particles while the force of the centrifuge pushes downward creating higher green densities. Regardless, the initial uniform distribution of *Pseudomonas syringae* is important.

B. *Pseudomonas syringae* as an ice nucleating template

Pseudomonas syringae, a previously unknown component of atmospheric clouds has been associated with the formation of cubic ice. Cubic ice was originally thought to be a very small percentage of the known ice on Earth. *Pseudomonas syringae* contains proteins that extend from the cell wall and act as nucleation sites for ice crystals that are responsible for initiating most forms of precipitation. Atmospheric scientists now believe

that this bacteria is responsible for initiating rain and snow[14]. Due to the lack of concentrated templating sites, cubic ice embryos do not reach a critical size and are thermodynamically converted to their more stable hexagonal form. The protein templating effect of bacteria has a profound effect on the thermodynamics of water and ice.

The *Pseudomonas syringae* bacteria used in this research was a product called Icemax™ from Johnson and Johnson Corporation. The *Pseudomonas syringae* is coated in sodium sulfate decahydrate, (Icemax™) according to the manufactures, increases the bond cohesion between ice layers[15]" yielding a more durable ice surface. To confirm that sodium sulfate decahydrate encapsulated the *Pseudomonas syringae* bacteria, an XRD pattern was taken (Figure 3).

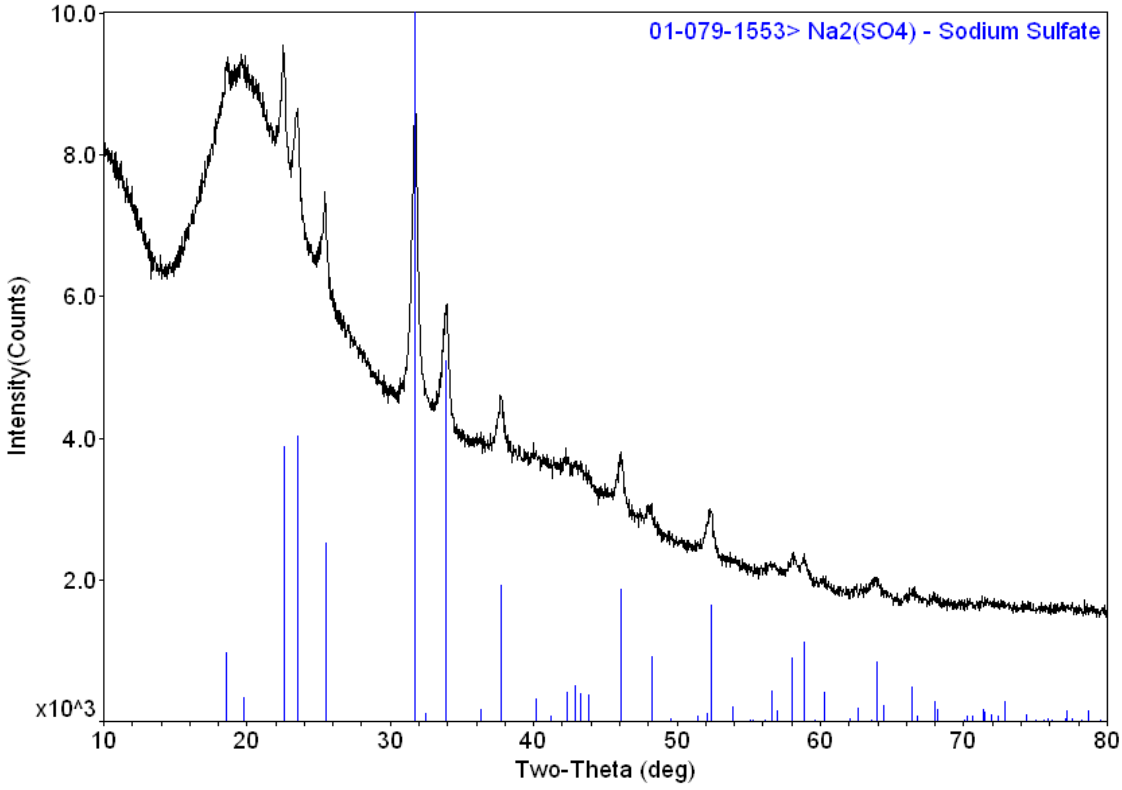

Figure 3: X-ray pattern of Icemax™ indicating the presence of sodium sulfate decahydrate.

Pseudomonas syringae acts as a template for ice formation using the protein that extends from the cell wall[16]. These templates are divided into three classes corresponding to the following temperature regimes: Type I, -5°C and above, Type II, -5 to -7°C, and Type III, -7 to -10°C[17]. *Pseudomonas* is the primary ice forming genus in the environment. Others include Erwinia, Enterobacter, and Xanthomonas (Table 1).

Table 1: Ice Forming Bacteria Known to Date

Genus	Species	Type I, II, III Template
Pseudomonas	*syringae*	I[18]
	fluorescens	I[19]
	viridiflava	I[20]
	chlororaphis	II[21]
	putida	II[22]
	antarctica	I, III[23]
Erwinia	*herbicola*	I[24]
	ananas	III[25]
	uredovora	III[26]
Enterobacter	*agglomerans*	I, II[27]
Xanthomonas	*campestris pv. Translucens*	I[28]
	campestris	II[29]

The genes encoding Type I ice nucleation active (INA) bacteria, despite different species of origin, are quite similar and yield highly ordered membrane proteins. The INA bacteria surface distribution absorbs and orients water molecules. At sufficiently low temperatures water forms ordered layers accreting on the bacterium. Stable formation of ice occurs when a sufficient size, defined as the ice embryo, is reached. Freezing begins with small clusters of water molecules. If the cluster, called an ice embryo, is below a critical size the unstable ice embryo decays. However at the critical size, nucleation is favorable and an ice crystal will grow. Acting as impurities, the bacteria play an important role in the freezing temperature of water (Solute effect)[30].

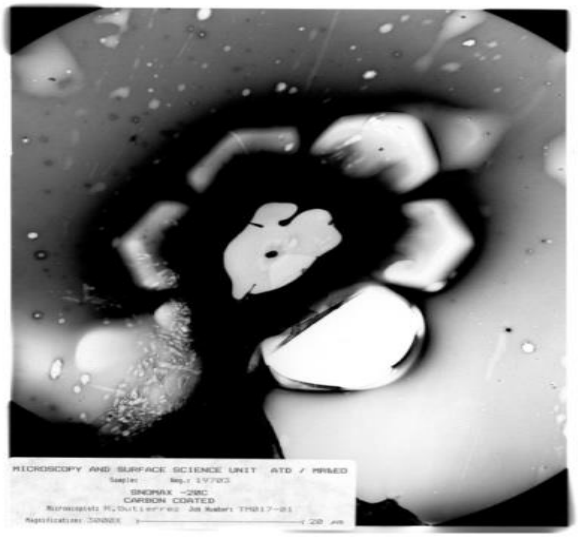

Figure 4: *Pseudomonas syringae* at the center of an ice crystal[31].

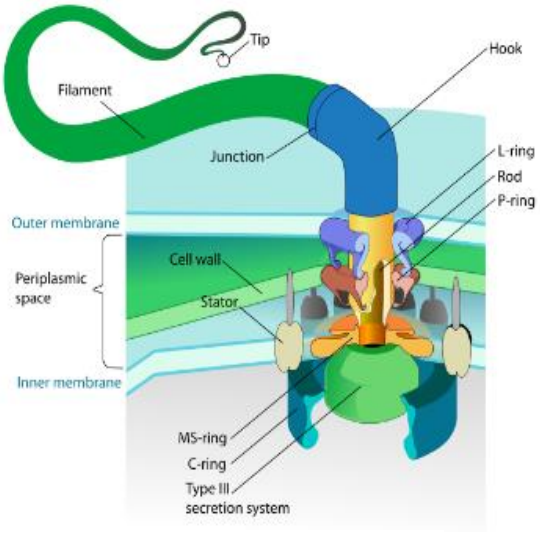

Figure 5: *Pseudomonas syringae* structure[32].

A *Pseudomonas syringae* bacteria at the center of an ice crystal as seen in an ESEM is shown in Figure 4. The ability of *Pseudomonas syringae* to promote ice formation comes directly from protein chains consisting of one or more polypeptides that extend from the cell wall as indicated in Figure 5. Polypeptides are linear polymer chains of amino acids bound together by peptide bonds between carboxyl and amino groups of adjacent amino acids. Proteins exist in the lowest kinetically attainable state of free energy. Non-polar amino acids are insoluble in water (hydrophobic); however, they are forced into water as part of the specific protein structure. By introducing hydrophobic groups, nearby water molecules become ordered which decreases the entropy of the system. The foreign particles act as a scaffold for crystal growth, a term deemed "ice embryo," by the *Encyclopedia of Surface and Colloid Science*[33]. "An ice embryo is formed within supercooled water by thermal fluctuations in contact with a liquid environment. Its growth is a matter of molecular reorientation involving breaking of water to water bonds in favor of the formation of water to ice bonds by overcoming the energy barrier, ΔG. " The outer membrane of the ice nucleation protein acts as an ice embryo (a template).

In order to form a critical ice embryo a negative free energy (ΔF_i^*) is required. In *Encyclopedia of Surface and Colloid Science* the free energy required for the formation

of a critical ice embryo is given by:

$$\Delta F_i^* = \frac{4\pi}{3}\left(\sigma_{i/w}\right)(r_i^*)^2 \quad (1)$$

Where $r_i^* = \frac{2\sigma_{(i/w)}}{\Delta H_{(i/w)}\rho_i ln\frac{T_o}{T_i}}$, is the critical radius, $\sigma_{i/w}$, is the ice-water surface tension, i/w means ice/water, ρ_i is the ice density, $\Delta H_{(i/w)}$the enthalpy of fusion, T_i the freezing temperature, and T_o is the absolute melting temperature of ice. The freezing process is calculated by the nucleation rate which is represented by:

$$J = Aexp\left(-\frac{\left(\Delta F_i^* + \Delta G^a\right)}{RT}\right) \quad (2)$$

Where A is a constant factor, ΔF_i^* is the critical free energy and ΔG^a is the activation energy required. The templating effect of INA bacteria lowers ΔG^a and thus enhances the formation of the ice embryos and associated ice at higher temperatures.

Another separate group of bacteria with similar proteins exists, called anti-freeze proteins (AFP). These proteins bind to ice surfaces and inhibit their growth. AFPs and antifreeze glycoproteins (AFGPs) depress freezing by adsorbing to the surface of the ice crystal and increasing the energy required for additional water molecules to orient themselves in the crystal lattice (hydrophobic aggregation). These may also have applications to processing, however implementation of AFP bacterium are beyond the scope of this research.

The main focus of this research is to determine how to use INA bacteria in a process where ceramic particles are incorporated into an ice matrix. The ice, which freezes at a higher temperature than normal due to the bacteria, yields a matrix with smaller preferentially oriented crystals. When transitioning from the liquid to the solid hexagonal phase waters density decreases and consequently its volume increases 9%. The phase diagram of ice/water exhibits a maximum density at 4°C. The subsequent decrease in density with the onset of freezing is sufficient to reduce the highest possible

green density leaving voids during sublimation. Figure 6 shows the density of water as a function of temperature.

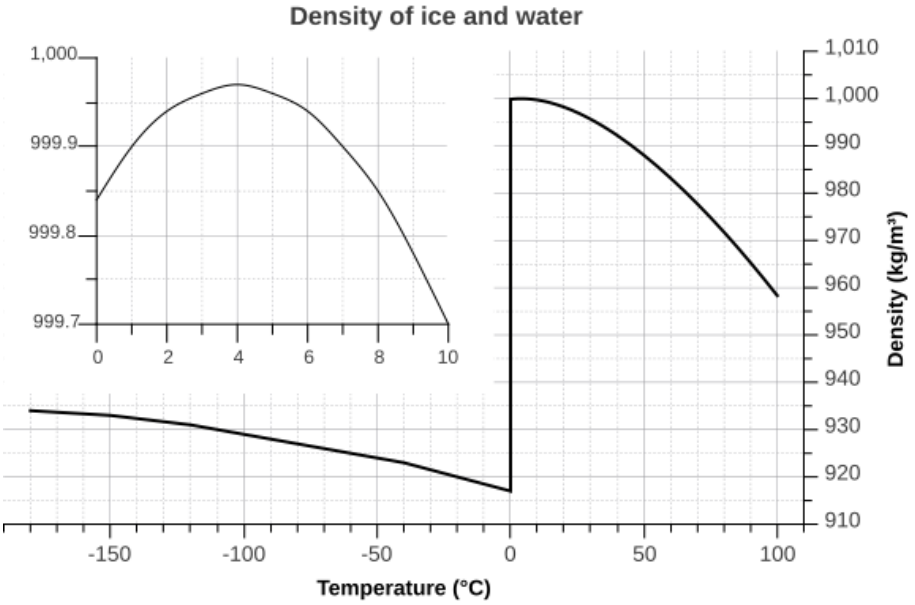

Figure 6: Density of water as a function of temperature[34].

Incorporating *Pseudomonas syringae* may reduce volumetric expansion by favoring denser ice formation at higher temperatures. It is expected that the process of forming a piezoelectric part due to the rigidity of the ice can then be subsequently sintered to form a near net shape ceramic component.

C. Piezoelectric materials and the 32 crystallographic point groups

Commercial piezoelectric parts have stringent requirements on porosity and homogeneity. Lead zirconate titanate, $Pb(Zr_xTi_{1-x})O_3$, has numerous practical applications. Lead zirconate titanate is a piezoelectric ceramic with a perovskite structure and a general formula $Pb(Zr_xTi_{1-x})O_3$ $0 \leq x \leq 1$, Figure 7. A perovskite structure consists of the general formula ABO_3, where A and B are cations[35]. Perovskites are the most common family of piezoelectric ceramics in use today. Discovered by the Curie brothers in 1880, direct piezoelectricity produces a surface charge as a result of an applied mechanical stress. The name "piezo" is from the Greek meaning "to press." It is the

primary coupling effect between electric and elastic phenomena[36].

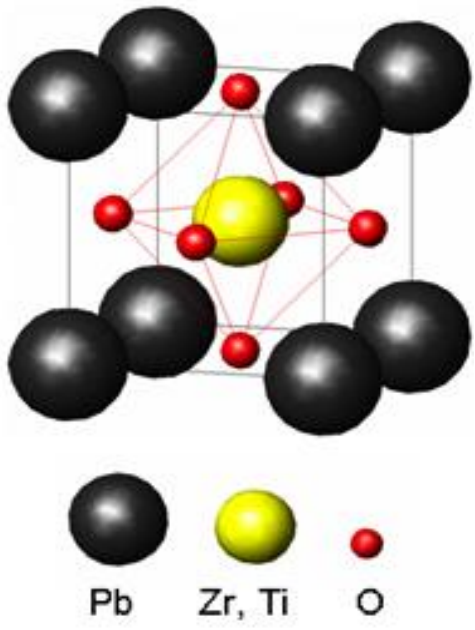

Figure 7: Atomic positions shown are the time-averaged positions for the cubic prototype material. Pb[0,0,0], O[1/2,1/2,0], Zr,Ti[1/2,1/2,12/] [37].

Of the 32 point groups, 21 are acentric and all but one of these are piezoelectric. Physical properties of the 20 piezoelectric groups can be described by tensor notation. Since physical properties mimic the underlying symmetry (Neumann's Law), only 20 of the 32 point groups permit piezoelectricity. However, this is relevant to the single crystal and not the polycrystalline situation. In order for a polycrystalline material to be usefully piezoelectric, it must be polar and reorientable (polable), i.e., a ferroelectric. This constraint reduces the permissible symmetry groups to 10.

The development of a polarization under an applied stress is defined as the direct piezoelectric effect. The linear relationship can be defined by the tensor equation $P_i = d_{ijk} T_{jk}$ where P is the induced polarization, T is the stress and d is the piezoelectric modulus defined as $d_{ij} = \left(\frac{\partial D_i}{\partial T_j}\right)^E$. A second effect called the converse effect is also observed when an applied electric field produces a strain, $S = dE$. These effects are shown in the Heckman Diagram given in Figure 8.

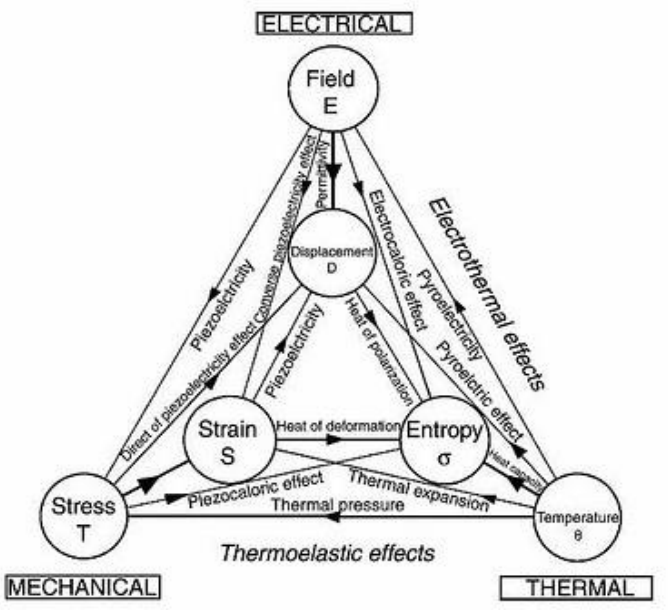

Figure 8: Heckmann diagram[38].

The 10 polar point groups have one or more possible polarization directions, i.e., 8 for 3m and 6 for 4mm. These represent the possible directions of poling, the resultant directions of polarization, for any given crystallite or domain within a polycrystalline ceramic. Since the macroscopic polarization is the summative response of the crystalline/domain polarization, the more "poling" directions available, the better the final poling and properties. $Pb(Zr_xTi_{1-x})O_3$ has two stable ferroelectric phases, rhombohedral and tetragonal. Consequently, crystallite domains near the 52:48 composition can be poled to either set of phase axes. The 14 possible directions yield greater response (8 rhombohedral, 6 tetragonal). This is proposed as one of the reasons that $Pb(Zr_xTi_{1-x})O_3$ is the primary piezoelectric ceramic in commercial use.

Lead zirconate titanate, $Pb(Zr_xTi_{1-x})O_3$, ceramics were initially used for naval applications where they are commonly referred to by their codes, NAVY-I, NAVY-II, NAVY-III, (Mil Spec 1376A,B[39]). The NAVY-I material is applicable to medium power acoustic radiation applications for sonar and ultrasonics and exhibits low mechanical and dielectric loss. Table 2 indicates characteristics of NAVY-I powder used commercially and in this work.

Table 2: Typical Characteristics of the NAVY-I Powder Commercially Used

Characteristic	Value
Granule Size (μm)	75-225 μm
Surface Area (m^2/g)	0.83 ± 0.01 m^2/g
Purity (%)	99.997
Color	Tan

D. Common forming techniques

Traditional ceramics are formed using three common techniques, near net shape forming, slip casting and injection molding. These techniques suffer from additions of sintering aids, and density gradients which diminish final sintered density. Injection molding is often expensive and involves high pressure. Therefore, CBFC has the potential to become a useful new technique due to its low cost, ease of use, and avoidance of binders.

i. Near Net Shape Forming:

High solid loading suspensions are required for near net shape formation. Particle contact is also necessary for full densification to occur by solid state diffusion and grain growth[2]. Typically a materials' diffusion behavior will in turn determine its sintering behavior. However, commonly practiced techniques involve the addition of sintering aids which can lower temperature and green density requirements. Although the benefits of all near-net shape forming are identical, the three common methods differ.

ii. Slip Casting:

Slip casting is a common processing technique that is widely used for the production of porcelain toilets and refractory crucibles as well as many other products. Slurry concentrations range from an average of 20 – 50 volume percent and binder may or may not be used. The process of slip casting involves the preparation of a suspension

which is highly dispersed. Typically a suspension is ball milled and then poured into a micro-porous mold[15]. The mold is generally made from plaster, which is formed by the reaction of gypsum and water. This method allows for varying degrees of porosity to be formed. The micro-pores in the material create strong capillary forces which draw water out of the suspension and deposit particles on the mold surface. As the deposit thickens, capillary forces are reduced and this can lead to undesirable density gradients. Since pores and gradients are ubiquitous, slip casting is not suitable for use of electroceramics, where either flaw would lead to catastrophic failure.

iii. Injection Molding:

The injection molding process starts with a high viscosity suspension with high binder concentrations. The suspensions are difficult to mix and often require expensive equipment with high torque capabilities. The suspensions are then injected into a metal mold at high pressures[15]. The use of high pressures and temperatures require the use of expensive metallic dies that are difficult to make. Consequently, injection molding is not an economical processing route for prototypes or small-number production.

iv. Centrifugal Bio-freeze Casting

CBFC of ceramic parts has potential to produce complex near net shape ceramic products. In its most basic form, freeze casting involves the freezing of a suspension in a solid mold. The second step is to remove the near net shape piece from the mold. A sublimative drying and removal of the aqueous medium under vacuum produces a green body ready for sintering. This simple process requires no complex tooling or toxic chemical additives. The process uses little or no binder and can be done quickly. The freeze casting process is very attractive on an industrial or prototype scale.

Methods and Baseline

This proof of principle work explains the preparation of $Pb(Zr_xTi_{1-x})O_3$ components via CBFC. The viability of the centrifugal freeze casting system for the production of dense $Pb(Zr_xTi_{1-x})O_3$ components was examined. In all experiments NAVY-I powder was used with a measured density of 7.84 g/cm^3. Icemax™ or more recently Snowmax™, *Pseudomonas syringae,* and $Pb(Zr_xTi_{1-x})O_3$ were examined in detail using techniques of XRD and ESEM.

A. Environmental scanning electron microscopy

Samples of Icemax™ were viewed under the ESEM. Using a Peltier stage, deionized water was sublimed by reducing the chamber pressure and then re-deposited by increasing the pressure. The bacteria were encased in sodium sulfate decahydrate was examined as well as the NAVY-I powder. NAVY-I powder supplied by Lockheed Martin was examined in an ESEM. The powder in Figure 9 exhibits normal granule characteristics and is not responsible for the unusual cubic ice formed during the CBFC process.

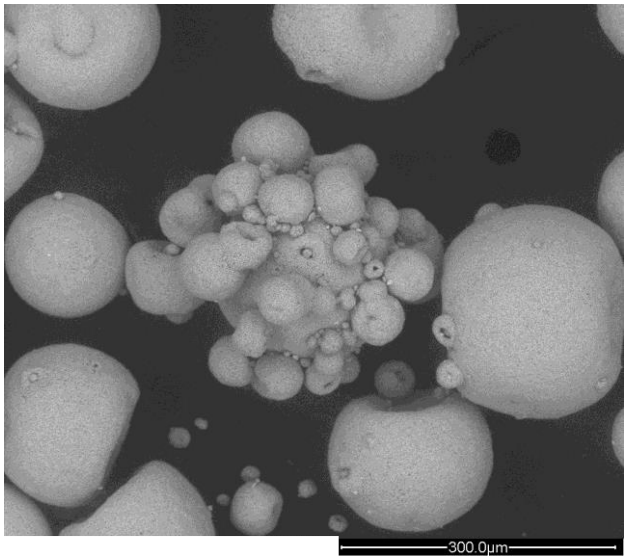

Figure 9: As received, NAVY-I spray dried powder, back scattered electron mode, with an original instrument magnification of 200x.

Pressure and temperature modifications were performed on an Icemax™ pellet (nominal mass 1 µg). At 1°C with an accelerating potential of 10 KeV, pressure of 3.40 Torr, the sample began to drift from the field of view, this indicated a change in shape of the structure with considerable pore structure developing as the pressure was reduced to 2.80 Torr. The pellet was collapsing slowly. The temperature was increased to 55°C in an attempt to drive off water; however, the structure was very resistant to sublimation and retained water at high temperatures. A second experiment shown in Figure 10 was conducted. Initially the sample was examined at 5°C, pressure 4.6 Torr with a beam strength of 15 KeV. The pressure was reduced to 0.4 Torr while the temperature was increased to 10°C. The fiber-like strand (Figure 10) began to contract. At 15°C "skeletonization" was starting to become apparent (Figure 11). Water was being removed from the sample. The temperature was increased to 40°C and pressure further reduced to 0.08 Torr. The sodium sulfate decahydrate was resistant to water loss. More surface roughening was observed with a small decrease in volume.

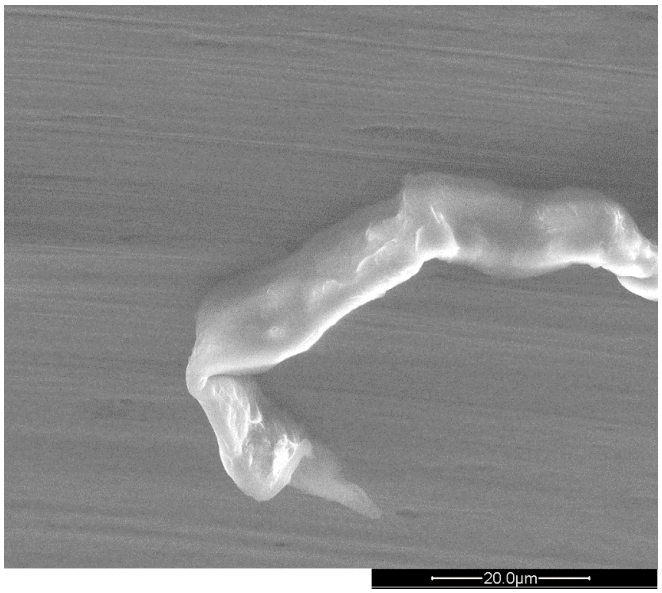

Figure 10: Sodium sulfate decahydrate with encased bacteria, original instrument magnification 3256x and pressure 0.40 Torr (53.32 Pa).

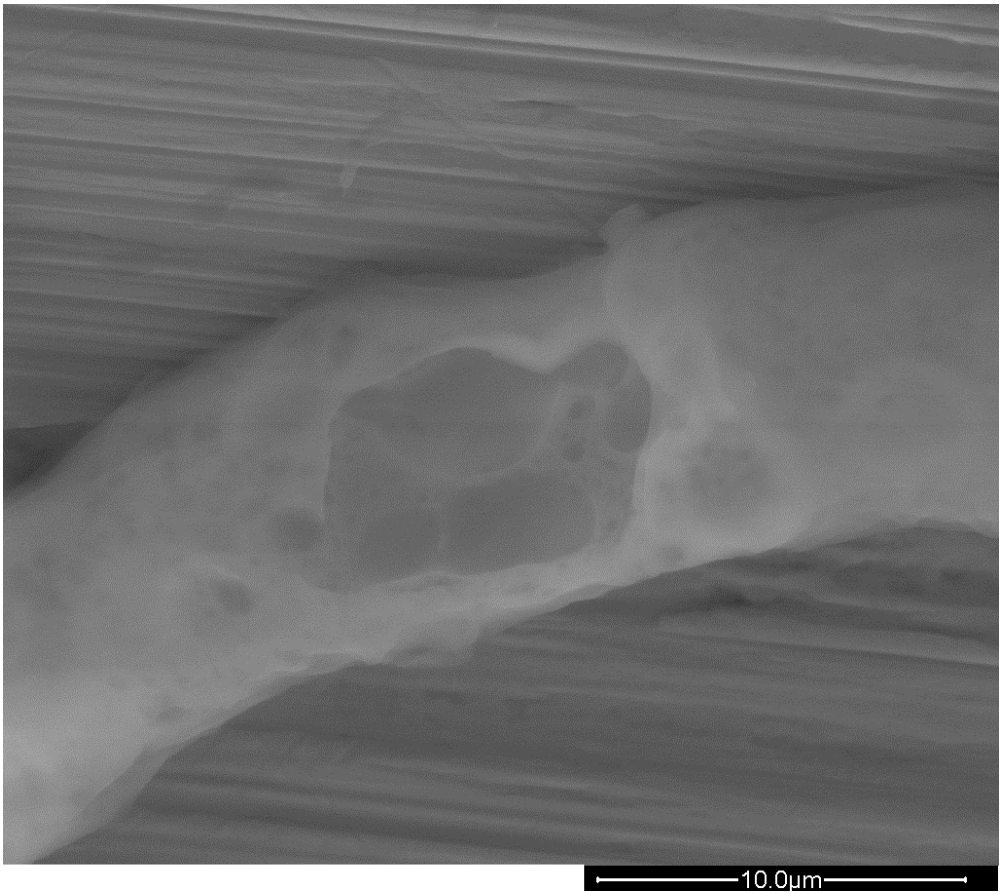

Figure 11: Icemax™, time elapsed, pressure reduced. Note for formation of holes, material is resistant to giving up water, original instrument magnification 10,000x and pressure 0.08 Torr (10.66 Pa).

Further work was done to isolate the bacteria; Figure 12 indicates the presence of the flagellum which is a distinguishing feature of *Pseudomonas syringae.* After looking at several sections of the pellet, *Pseudomonas syringae* is seen to form clusters which are responsible for effective ice templating behaviors for cubic ice (Figure 13). Consequently, ice produced with the aid of *Pseudomonas syringae* is a tighter grained and more uniform ice than that which is naturally produced. This was also observed by Johnson and Johnson Corp.[40].

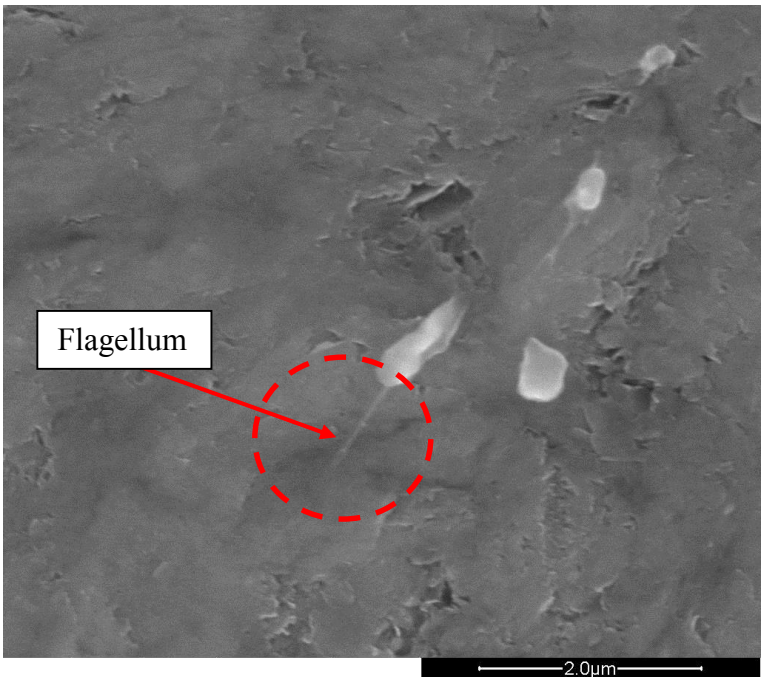

Figure 12: *Pseudomonas syringae* bacterium incased in sodium sulfate decahydrate, note the flagellum.

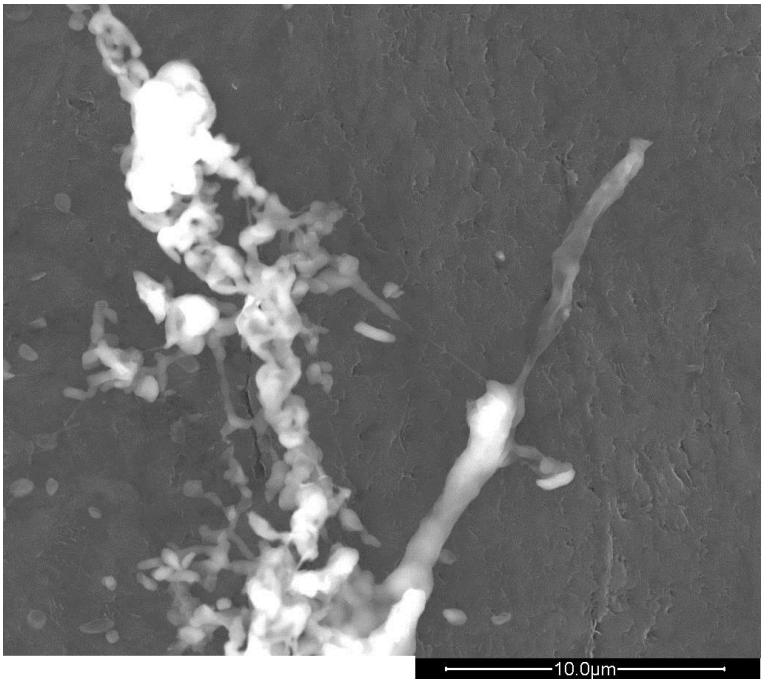

Figure 13: Clustered bacteria, necessary to form an ice template large enough for an embryo to form.

B. *Pseudomonas syringae* ice formation

To determine the ability of the bacteria to form ice, plastic sample communion cups (6 ml) filled with one drop of deionized water and one Icemax™ pellet (nominal mass 1 µg), were placed in 9 distinct areas inside a Sigma Systems Corp. cooled environmental chamber. The chamber was fitted with a liquid nitrogen tank and was cooled by increments of 1° Celsius. The system was then allowed to equilibrate for 10 minutes. A Type K thermocouple was used to measure the temperature of the sample cups. At each degree of cooling, the cups were quickly removed. Upon visual inspection, if the drop was frozen, it was remelted and additional drops were added. This was repeated until the cups were full (~120 drops) or visible liquid was present after thermal equilibration. Evidence of the bacteria's ability to promote ice formation leads directly to the preparation of the slurries.

C. Water Compatible Binders

Following an investigation of the spray dried NAVY-I powder, and *Pseudomonas syringae,* freeze forming slurries were created with additions of one of three water compatible binders: polyethylene glycol (PEG), polyvinyl alcohol (PVA), and polyglycolic acid (PGL). The monomers of these common binders are shown in Figure 14.

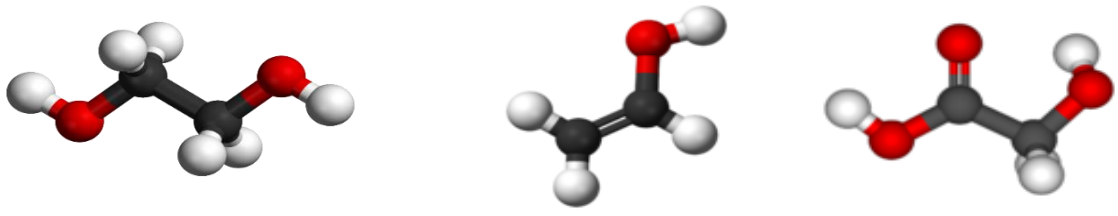

Figure 14: Ball and stick structures of monomers for PEG, PVA, and PGL[41].

Figure 15 shows vials with additions of common binders after freezing[42]. Additions of PEG, PVA and PGL were found to inhibit the formation of large ice crystals. The combination of PVA and PGL was particularly effective at preventing the formation of large ice crystals. PEG had the least effect on ice formation and is not a viable additive for slurry preparation

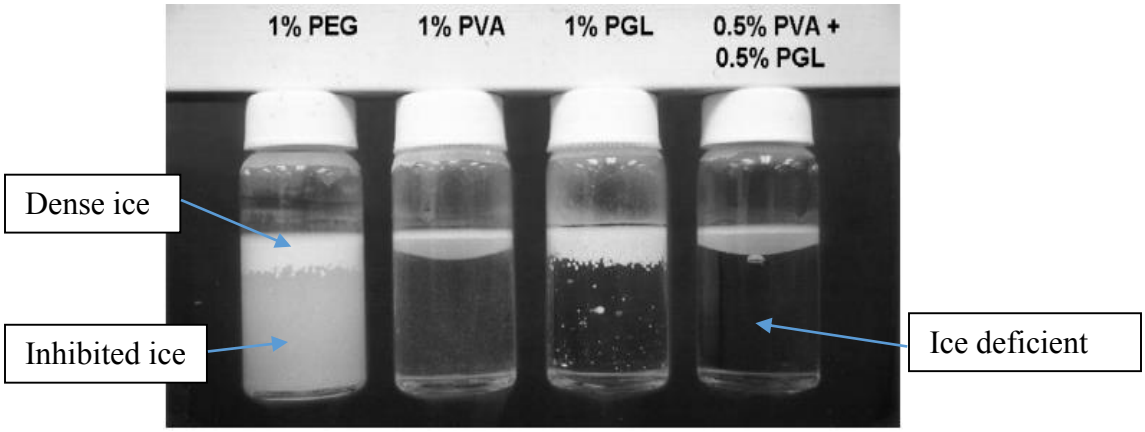

Figure 15: Polymer ice formation inhibition, Patent 6,616,858 B2[42].

D. Freeze Forming

Slurries were prepared using 20 g of water, bacteria and 30g of $Pb(Zr_xTi_{1-x})O_3$. The compacts were prepared by directly placing the powder into the bucket firstly followed by deionized water and then the bacteria. No mixing was necessary as the water uniformly coated the samples. The powder, water and bacteria were loaded into empty aluminum 750ml buckets that were designed to be centrifuged in the Marathon 21k centrifuge. NAVY-I powder and water were added systematically (Table 3) until an appropriate ratio was visually determined where the powder was coated fully in water without excess. Additions of controlled levels of common binders, PEG, PVA and PGL were added. Sample compositions were prepared including those with and without binder (Table 3).

During centrifugation the speed was set to 5,000 rpm as suggested by the manual (Fisher Scientific). However, the actual speed varied. The true speed never exceeded

4,800 rpm but dropped to 4,200 as a result of the cooling process. The bearing grease, when cooled below 4°C, begins to thicken and creates drag which slows the arm speed. The samples were cooled slowly to -5°C as a precautionary measure. While evidence suggests the samples were solid at 0°C, due to the long process time in excess of 15 hours, it was better to ensure the samples were cooled below their transformation temperature.

Table 3: NAVY I, Water, Bacteria and Binder Optimization (centrifuged 15 hrs; 0°C)

NAVY-I Powder (g)	Deionized Water (g) (with 5 µg bacteria)	Binder Additions (by volume percent) Four compacts per composition				Comments
		PEG	PVA	PGL	NONE	
5	45	1	0	0	0	Ring formed is too thin
		0	1	0	0	
		0	0	1	0	
		0	0	0	0	
10	40	1	0	0	0	Ring formed is too thin
		0	1	0	0	
		0	0	1	0	
		0	0	0	0	
15	35	1	0	0	0	Compact is “fragile”
		0	1	0	0	
		0	0	1	0	
		0	0	0	0	
20	30	1	0	0	0	Ratio is optimal
		0	1	0	0	
		0	0	1	0	
		0	0	0	0	
25	25	1	0	0	0	Compact is “soggy”
		0	1	0	0	
		0	0	1	0	
		0	0	0	0	
30	20	1	0	0	0	Compact breaks apart
		0	1	0	0	
		0	0	1	0	
		0	0	0	0	
35	15	1	0	0	0	Powder does not stay compacted
		0	1	0	0	
		0	0	1	0	
		0	0	0	0	

It was found that additional binders such as PEG, PVA, and PGL negatively impact the formation of desirable ice by binding to the templating sites of the bacteria. For this reason the use of additional binders was abandoned. Additional samples produced were centrifuged at 4800 rpm and stored in a freezer until they could be vacuum-assisted dehydrated. Figure 16 denotes the [111] direction which is the preferential direction of ice formation inside the centrifuge buckets.

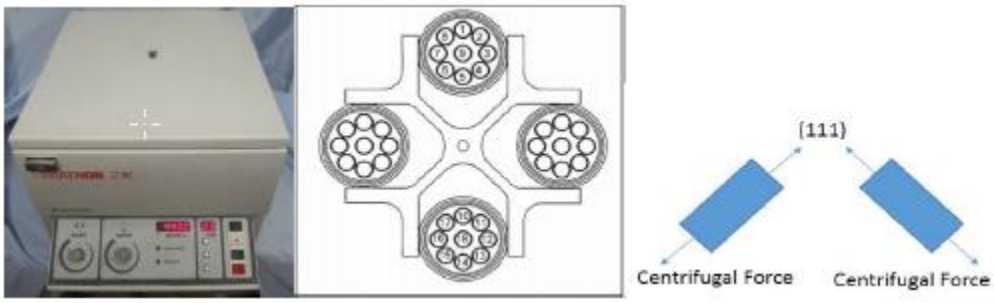

Figure16: Marathon 21K centrifuge.

Compaction in a centrifuge is commonly reported in gravities "***g***"

As excess ice forms during the process, it acts to further compress the compact, by applying a secondary downward pressure. The total force exerted on the compact is approximately 1350***g*** (Eqn 6). This is calculated using the arm length of the centrifuge and midpoint of the cup.

$$\omega = 4800\ rev/\min = 502.655\ rad/sec \quad (3)$$

$$r = midpoint\ of\ bucket = \frac{1}{2}L = \frac{1}{2}(0.1047m) = 0.0524m \quad (4)$$

$$a_c = \omega^2 r = (502.655)(0.0524) = 13230\ m/s^2 \quad (5)$$

$$Centripetal\ acceleration = \frac{13230 ms^{-2}}{9.8 ms^{-2}} = 1350\mathbf{g} \quad (6)$$

The centrifuge and premade chamber are initially precooled with the aid of liquid nitrogen to speed the cooling process. The chamber takes more than four hours to cool to the appropriate temperature range described later without precooling. The centrifuge was a Marathon 21K which was housed in a temperature controlled box lined with aluminum

foil and situated between two refrigerator compressors as shown in Figure 17.

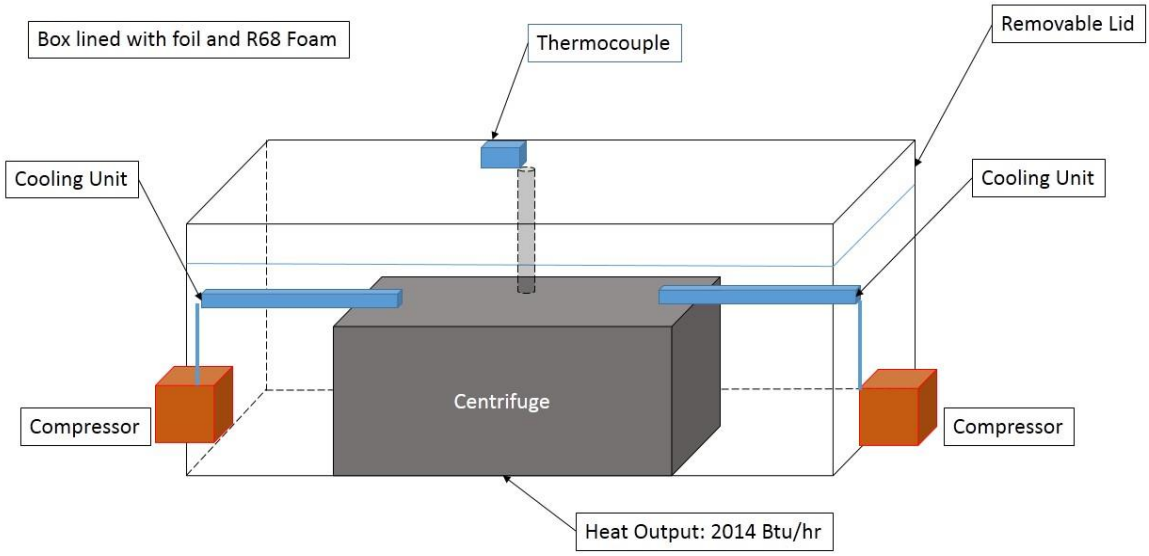

Figure 17: Chamber and centrifuge cooling setup.

The centrifuge chamber was cooled in an insulated crate. The interior was lined with aluminum foil which is effective at blocking incoming heat. Isolation foam was added under the centrifuge unit. A small hole was drilled in the top of the box to allow for a Type K thermocouple. The thermocouple measures tenths of a degree (Thermoworks[43]). Two compact compressors were placed outside the box and holes allowed the cooling to the centrifuge. Over the duration of the 15 hour time period the centrifuge unit generates heat. A temperature of -5°C could be maintained for a limited time; however, after extended hours, the cooling chamber temperature rose above zero degrees Celsius.

E. Construction of the chamber for vacuum-assisted dehydration

A vacuum-assisted dehydration chamber was constructed from 4 inch diameter steel pipe. A ¼ inch pilot hole for a thermocouple was drilled in the center the chamber and sealed with vacuum grease. A stage which can hold one sample was mounted in the center of the chamber and vacuum barbs were added with the aid of a tap and die set. An

external copper collar was constructed which fit around the chamber. Copper coils were added to allow for temperature controlled water to flow through the collar equally heating the chamber. The design of the vacuum-assisted dehydration chamber was modified from a presentation by Kinetics Thermal Systems entitled Theory of Freeze-Drying, Figure 18.

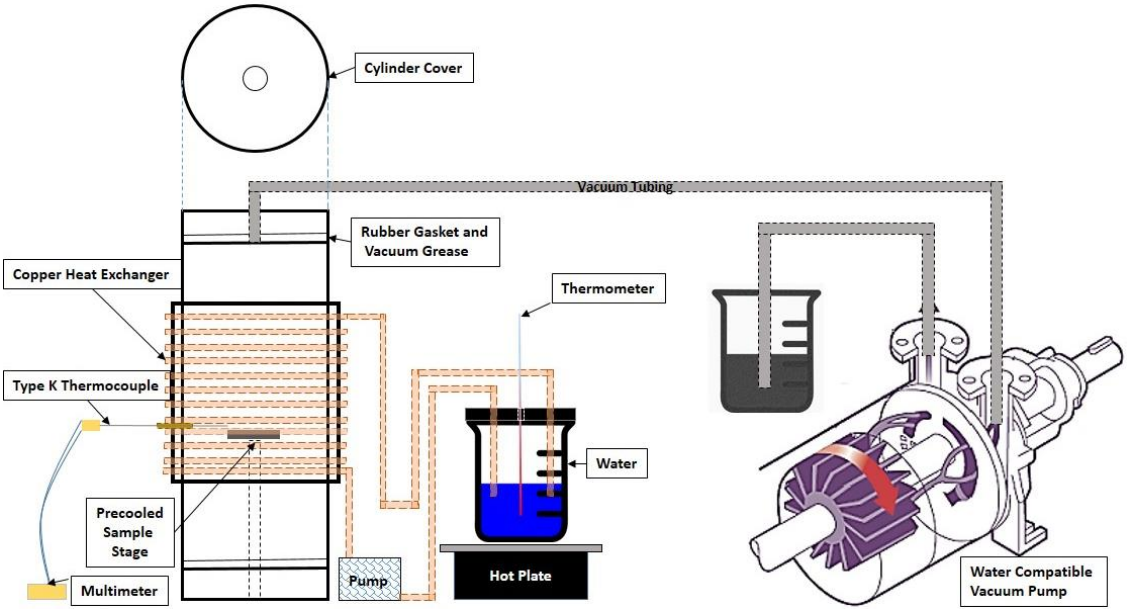

Figure 18: Chamber for vacuum-assisted dehydration.

The water pump for the system was a Swiftech, MCP355, capable of 22 psi nominal head pressure. The sample stage is initially precooled as suggested by the presentation. The water in the beaker was maintained at 72°C and the chamber 70°C. A roughing pump was used to draw a vacuum.

Results and Discussion

The results (Figure 19) show the effectiveness of the INA properties of *Pseudomonas syringae.* The coexistence of water and ice shows the non-equilibrium nature of the system, i.e., the *Pseudomonas syringae* nuclei only template a small volume and hence a higher density of nuclei is needed to crystallize the entire sample. This observation suggests an optimal ratio of bacteria to water is required.

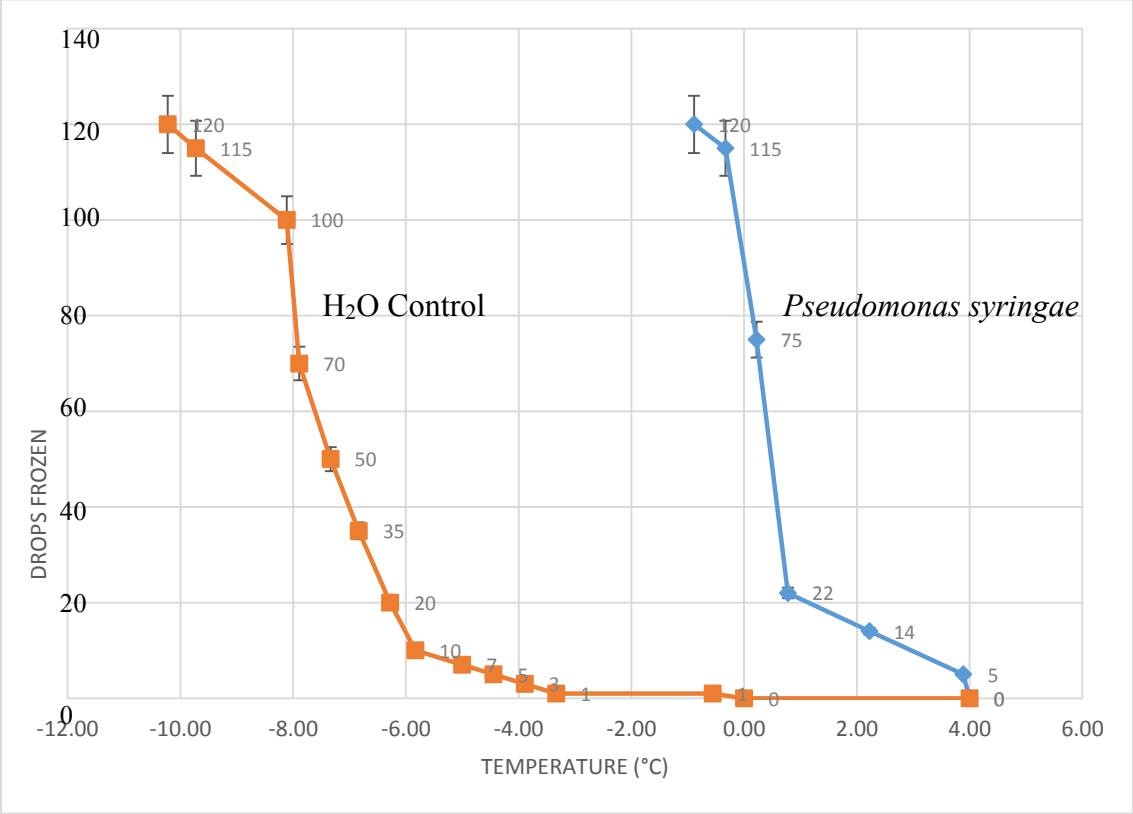

Figure 19: Number of drops frozen of H_2O without (left) and with (right) the presence of *Pseudomonas syringae* bacteria.

During the experiment a significant degree of undercooling was found i.e., the pure water system did not freeze at 0°C. This is attributed to the lack of nucleation sites for ice crystals. Deionized water in the absence of nucleation sites can be cooled to -

48.3°C without forming ice[44]. The size of the Icemax™ pellets varies greatly. According to the packet instructions, one packet weighing approximately 15 grams should be added to 250 gallons of water. A single pellet may thus weigh less than 0.00001 grams (1 µg). The presence of cubic ice was confirmed with X-ray diffraction performed with a sample frozen in a plastic X-ray diffraction sample holder, (Figure 20). Note that a strong preference for (111) growth perpendicular to the basal plane is apparent.

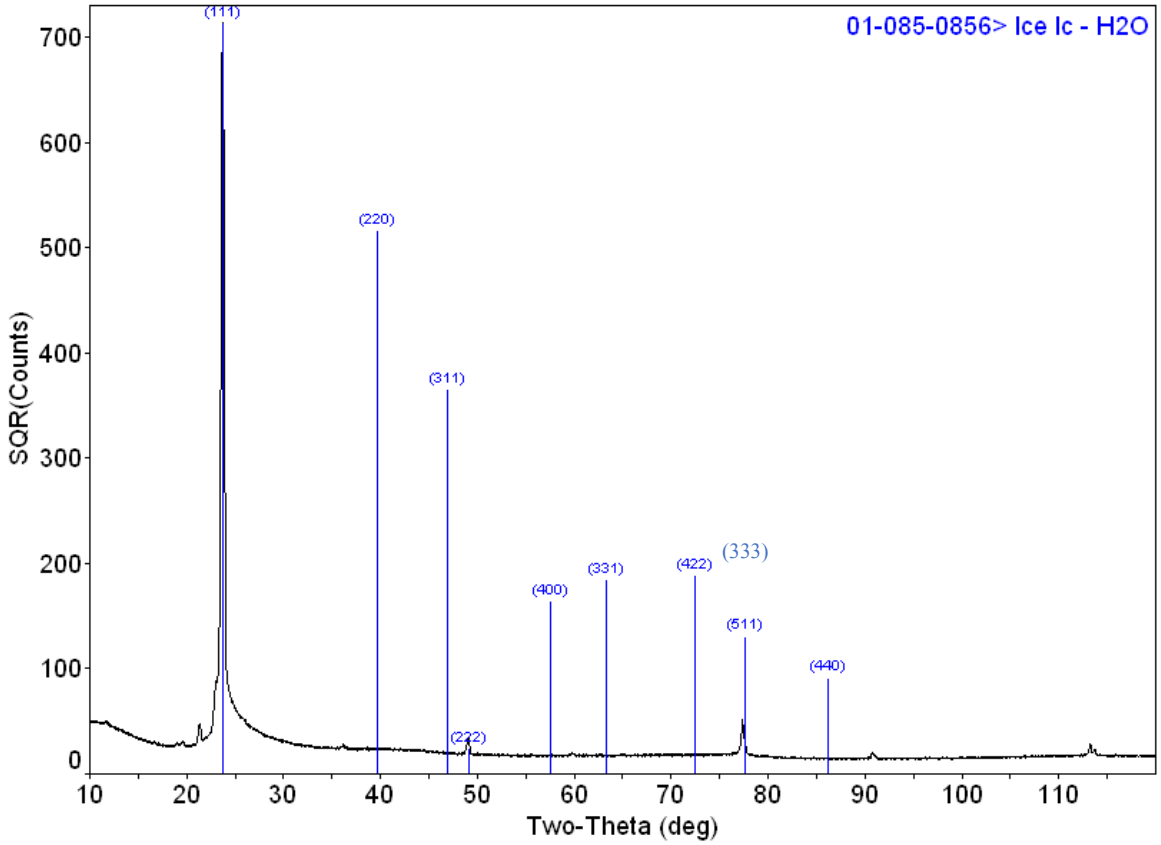

Figure 20: X-ray pattern of cubic ice formed with the aid of *Pseudomonas syringae* without centrifuging.

Some slight peak shifts were observed at larger 2θ degrees in Figure 20 due to melting of the ice while being X-rayed. Misalignment caused by the sample surface being lower than the stage is responsible for the shift[45]. Under normal conditions simple correction equations for sample displacement can be applied; however, due to the complexity of real time melting, corrections are difficult to account for. The intense peak

at (333) corresponds to the (511) peak identified by the XRD software. These occur at equivalent Bragg angles, $h^2 + k^2 + l^2 = 27$, for cubic systems.

Figure 21 shows the diffraction pattern of hexagonal ice. There are two additional peaks at 22° 2θ and 25° 2θ not present in cubic ice.

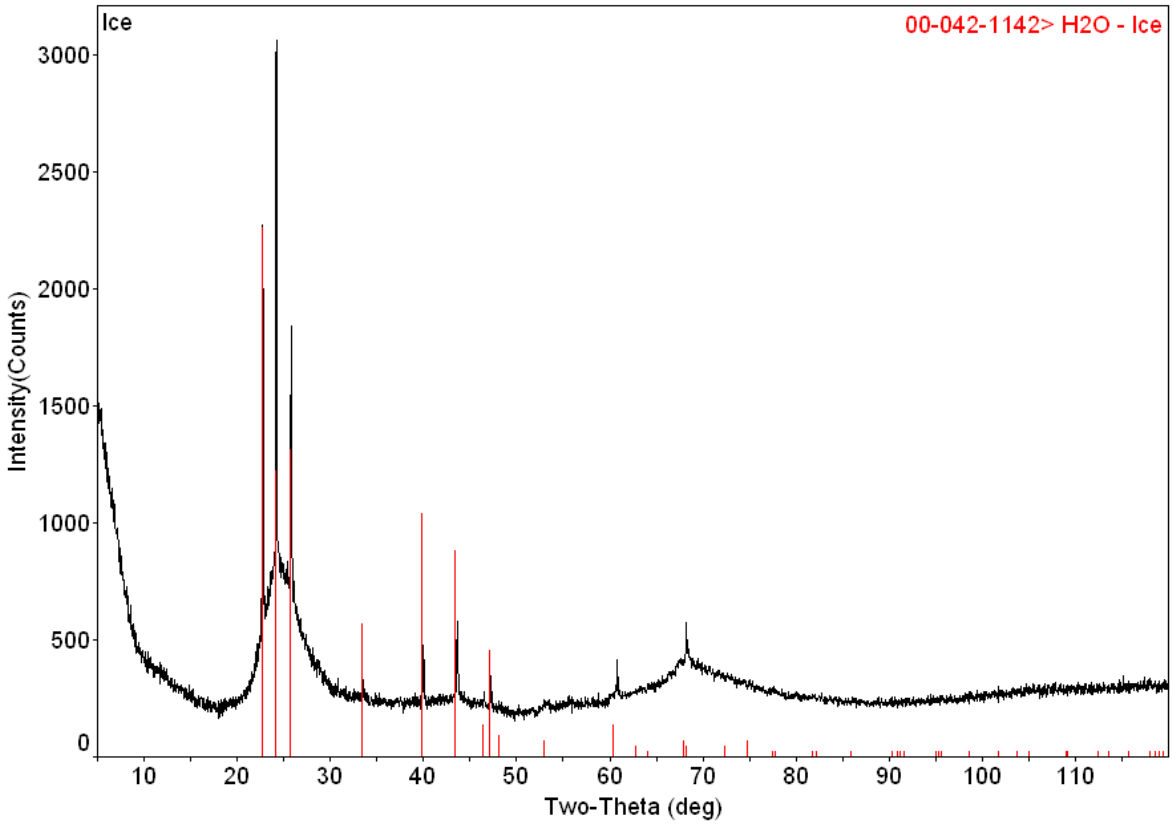

Figure 21: X-ray pattern of normal hexagonal ice.

The formation of cubic ice with the aid of *Pseudomonas syringae* leads to higher green density compacts because the density of cubic ice is greater than that of hexagonal ice, 0.92480 g/cm^3 versus 0.9167 g/cm^3 at 0 °C respectively. Figures 22 and 23 reveal a nearly fully dense green compact after centrifuging. This is evident by the lack of voids indicated by dark areas. Quantitative determination of green density is complicated by the formation of "excess" ice -- the frozen liquid excluded during centrifugation.

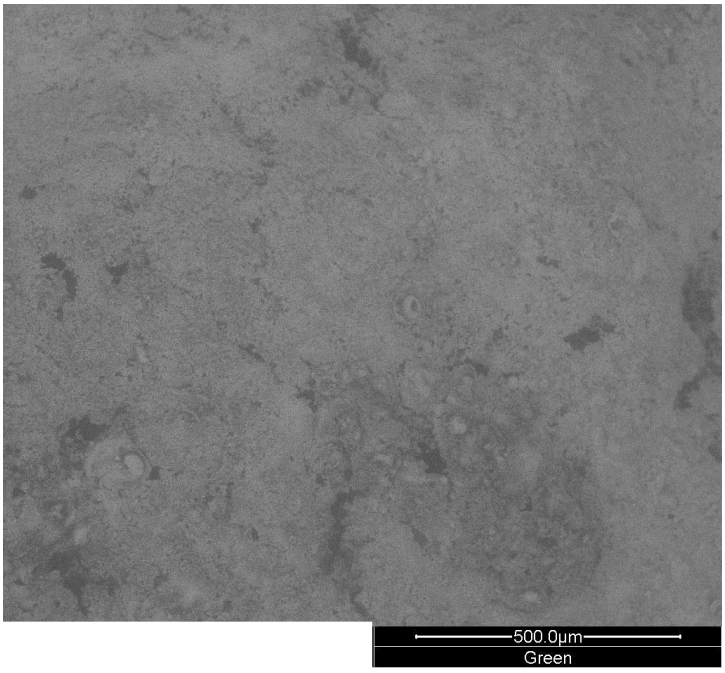

Figure 22: The dense surface of a centrifuged green compact, water bacteria and $Pb(Zr_xTi_{1-x})O_3$.

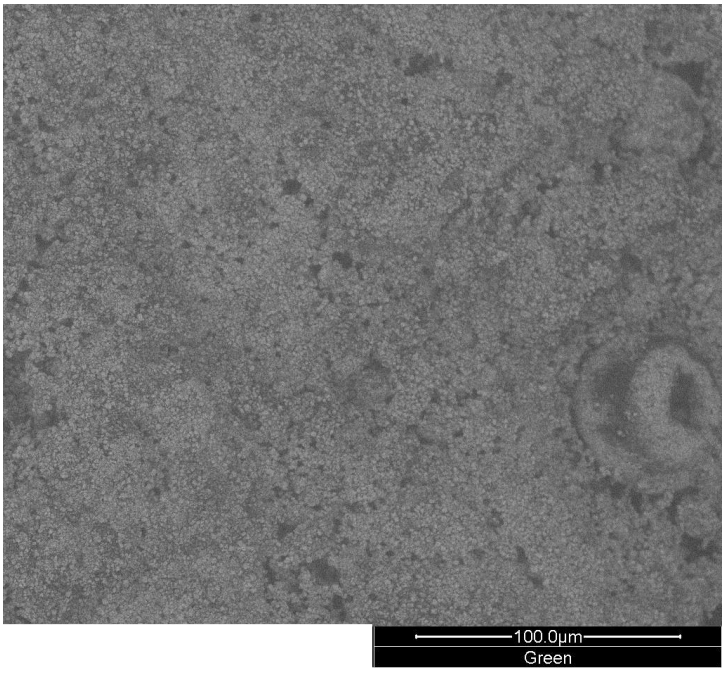

Figure 23: Dense surface of a green compact with a partially broken down spray dried granule.

Although the amount of excess ice was not quantitatively determined, it was approximately half the total thickness. Thus the powder: liquid ratios are nominal in Table 4 with high green densities.

Table 4: Vacuum-assisted Dehydration, Density, including Powder and Bacteria

Sample Number	Conditions (With Bacteria)	Nominal volume ratio % powder:liquid	Apparent dehydrated green density* as % of theoretical**
1	20 g powder, 30 g water 15 hr centrifuge, held at 0°C	7.81:92.19	~80
2	20 g powder, 30 g water 15 hr centrifuge, held at -1°C	7.81:92.19	~80
3	20 g powder, 30 g water 15 hr centrifuge, held at 0°C	7.81:92.19	~80

*Density calculated geometrically after vacuum-assisted dehydration, **7.84 g/cm^3,

The samples containing varying ratios of NAVY-I powder, water and bacteria were prepared as listed in Table 5. All were centrifuged at 4800 rpm for a time of 15 hrs (see also Table 3).

Table 5: NAVY-I Powder, and Water Combinations without Binder Addition from Table 3

NAVY-I Powder (g)	**Deionized Water (g) (with Bacteria)**	**Nominal Volume % Powder**	**Comments**
5	**45**	**1.39**	**Ring formed is too thin**
10	**40**	**3.08**	**Ring formed is too thin**
15	**35**	**5.17**	**Compact is "fragile"**
20	**30**	**7.81**	**Ratio is optimal**
25	**25**	**11.28**	**Compact is "soggy"**
30	**20**	**16.02**	**Compact breaks apart**
35	**15**	**22.89**	**Powder does not stay compacted**

Difficulty arose during sample removal. The samples were frozen directly in the steel buckets, therefore, removal was quite difficult. Partial melting from the bottom was attempted, but the strong adhesion properties left the compact stuck to the bottom of the buckets. Also, this method of attempted removal left the compact in a "soggy" state. A second attempt to remove the samples included using a thin metal spatula to pry the edges around the cup loose. While this method was somewhat successful in allowing the compacts to be removed, the edges of the samples were damaged (Figure 24).

Figure 24: Sample with damaged edges.

After a substantial number of empirical trials, a method to remove the samples was finally found. A non-lubricated Trojan condom stretched over the bucket was loaded with the appropriate amounts of water and powder. A small pin hole was placed in the condom to allow air to escape from inside the bucket as the condom formed a tight seal. This method creates a flexible barrier that can fill the container volume, but also can be easily removed. This method was mostly successful except for when the centrifugal force tore the condom. Once the samples were removed a secondary problem was discovered. The excess ice that formed above the powder sample was difficult to separate from the compact itself. This issue was resolved by using a plastic barrier that had a density greater than the water, but less than the powder. This plastic layer was

sufficiently porous/loose fitting that a small amount of ice could keep the compact connected to the excess ice, but allowed it to separate easily. The addition of a plastic barrier was a viable solution due to density arguments. According to data from thermogravimetric analysis, (TGA), excess binder, on basic principle of density difference, is separated during centrifugation. The PVA binder from the spray dried granules has a density of 1.19-1.31 g/cm^3, which falls between the powder and the plastic barrier, allowing for easy separation of the compact from the excess ice. This separation ability is further amplified by the inhibition of ice formation from PVA as noted earlier in the patent. Figure 25 shows a TGA of a NAVY-I powder indicating the presence of PVA binder with a melting point of 180-190°C for the partially hydrolysed grades followed by a burnout stage.

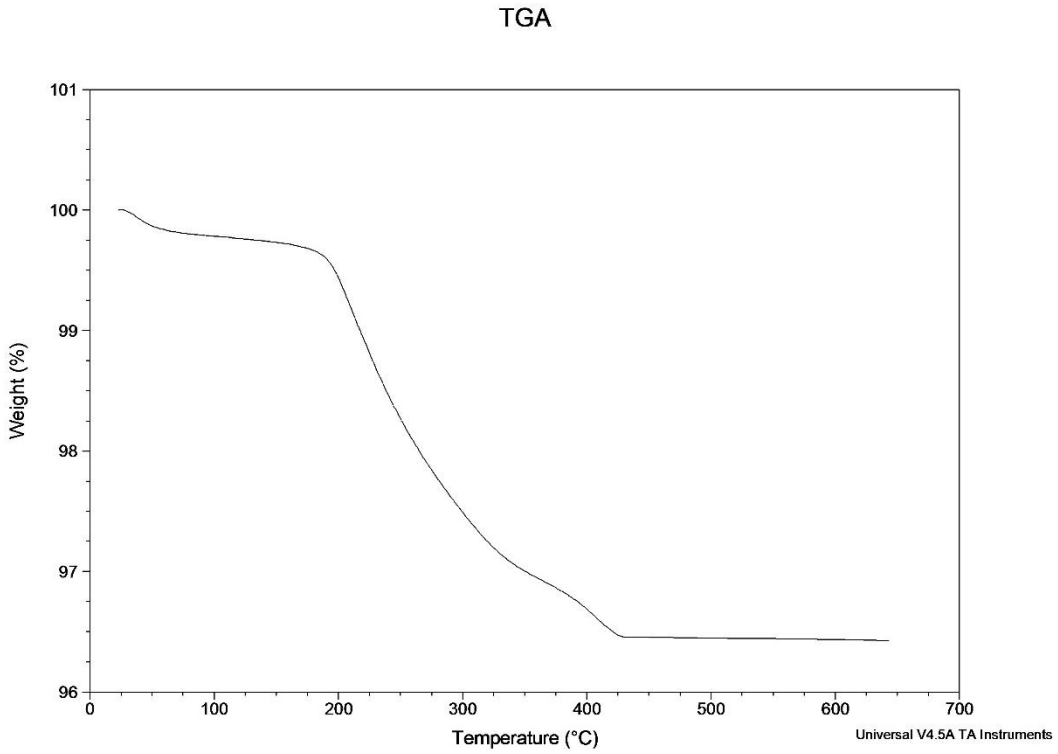

Figure 25: TGA of NAVY-I powder indicating approximately a 3% weight loss of PVA.

In Figure 26, TGA is performed on a vacuum-assisted dehydrated compact. There is less binder in the compact suggesting that excess binder separates to the interface as suggested earlier.

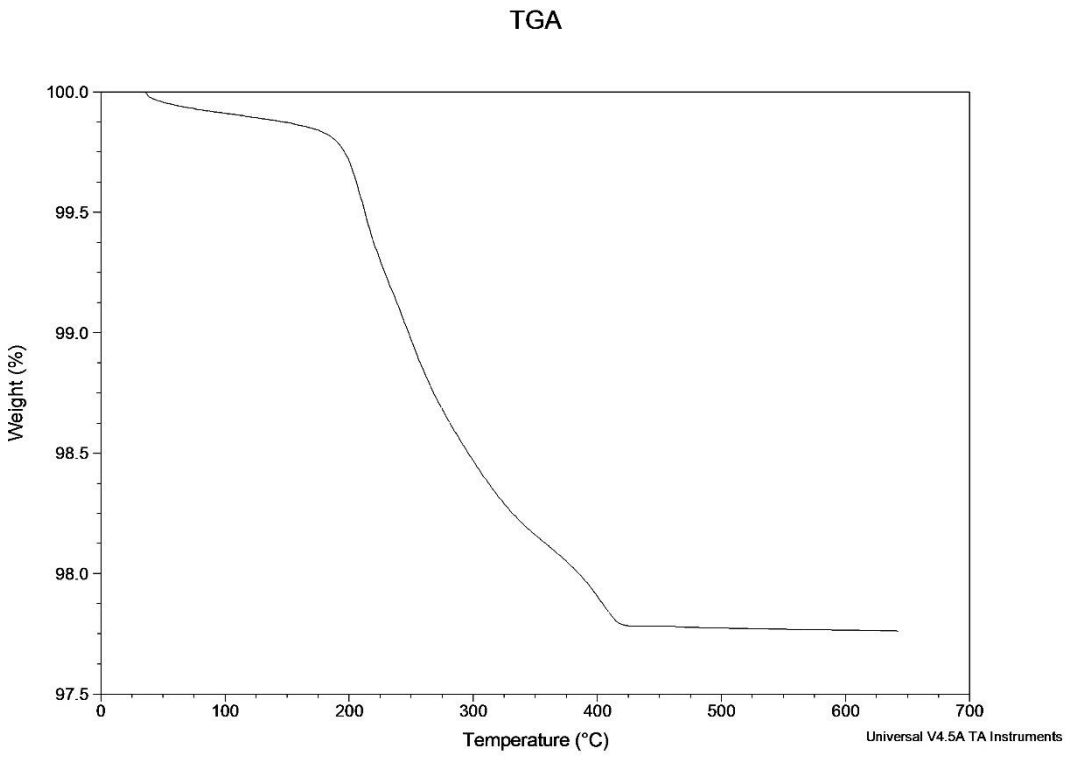

Figure 26: TGA of the vacuum-assisted dehydrated compact indicating approximately a 2% weight loss of PVA.

After the samples were removed, they were transferred to the vacuum-assisted drying chamber (figure 18), where the ice was allowed to sublime under vacuum. The dried samples (80% of theoretical), were then fired by a standard unoptimized firing schedule. A ramp rate of 100°C per hour to 800°C was used. A one hour hold at 800°C was also used followed by heating at the same rate, to 1300°C with a 2 hour hold at 1300°C. A lead(II) oxide donor pellet was present. Fired discs were cored, polished, and beveled by hand finishing.

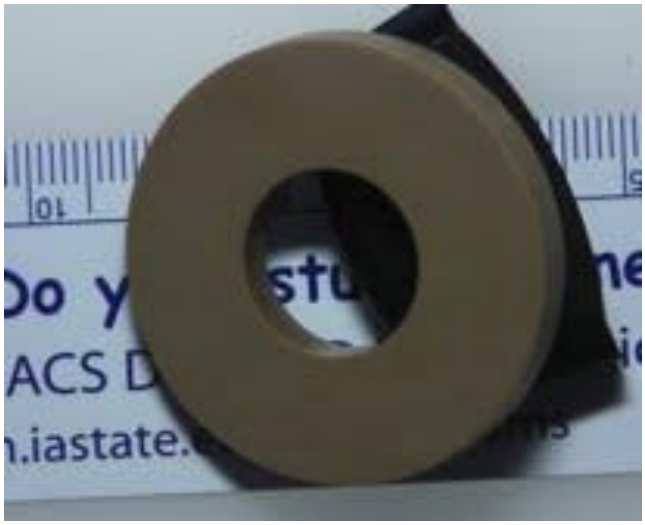

Figure 27: Un-electroded sample.

Samples were electroded by painting on a silver paste and allowing it to air dry. The electroded samples were tested in Delta Environmental Chamber under Labview™ computer control. The temperature was controlled via a Labview program and set to run from -50°C to 195°C. An HP 3488 multiplexer selects among the samples and an HP 4284 bridge records the capacitance which permits determination of relative permittivity from the geometry (Figure 28). A commercial NAVY-I poled sample from Morgan Electroceramics[46] was also tested.

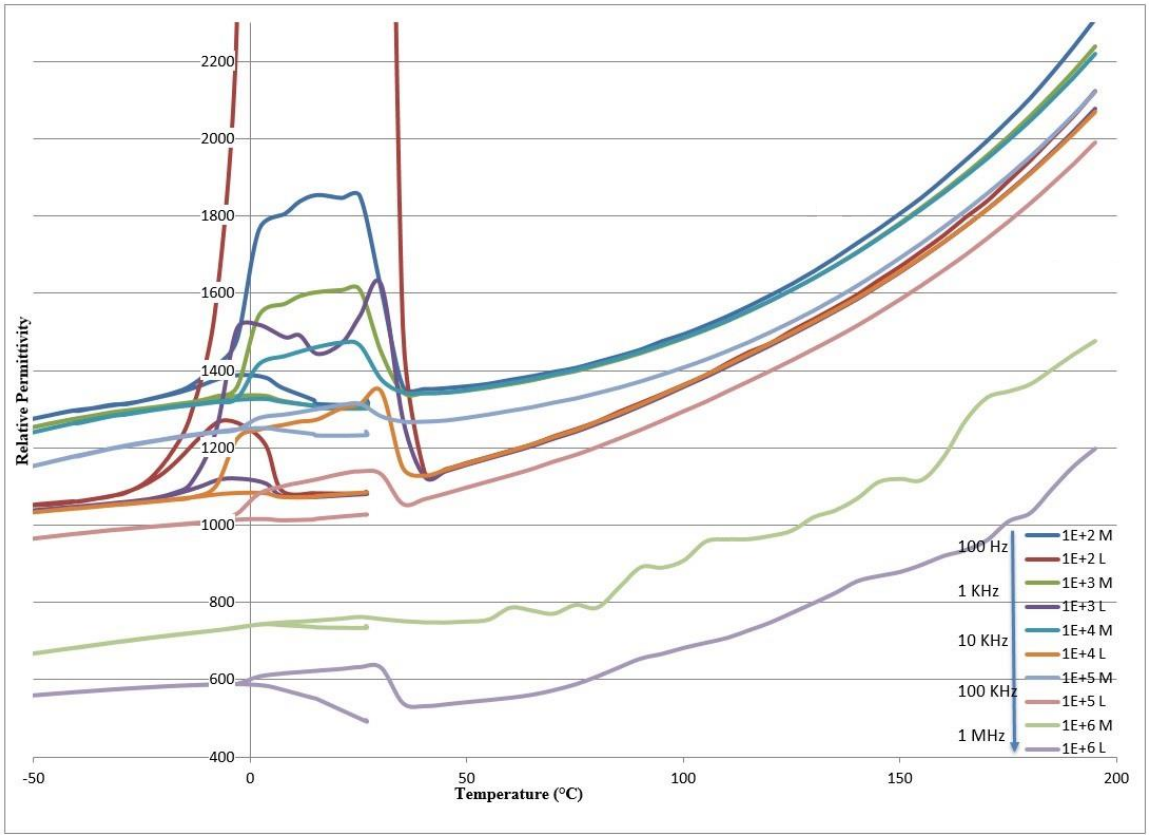

Figure 28: Relative permittivity as a function of temperature and frequency. The denotations L and M stand for Lamphier and Morgan.

The large loss peak observed near 0°C is due to water condensation and perhaps electrodes from the silver paste that were dried and not fully sintered. This peak has been arbitrarily clipped from the 100Hz data set to better show the materials performance. At all frequencies, samples produced by CBFC (L-Lamphier) were similar in performance to commercial poled samples produced by Morgan Electroceramics (M-Morgan). The unpoled nature of the CBFC-L samples, suggests the possibility of further improvement.

Conclusion

The adaptation of *Pseudomonas syringae* bacteria to centrifugal freeze casting provided finished pieces with densities greater that 96% of theoretical. Data for three fired samples are shown in Table 6.

Table 6: Final samples were prepared using Table 5 optimal conditions. The samples were centrifuged for 17 hours at 4800 rpm and cooled to -2°C with a dwell time of 1 hour and fired with the standard cycle

ID (mm)	OD (mm)	Thickness (mm)	ρ (assuming ρ_T = 7.84 g/cm^3)
15.56	37.58	4.87	>96%
15.49	37.8	4.89	>96%
15.62	37.43	4.92	>96%

Two samples were polished by standard techniques and electroded with air-dry silver paste prior to dielectric testing. The samples in Table 6 were not poled. The tested dielectric properties were equivalent to commercial poled samples. Sample repeatability is comparable as depicted by the diameters and densities in Table 6.

Overall, CBFC shows substantial promise. Samples of high density with excellent dielectric properties were achieved. Processing was completed above 0°C --i.e., within the performance specification of industrial equipment. In addition, the binders and solvents were aqueous-based and thus inherently environmentally friendly.

Future work

The production of complex shapes requires future work in order to yield dense final products. Adjustable ring sizes with inserts may be developed. These molds could be flexible materials or a porous bronze material which allows air to escape. Multiple part molds can also be suggested. The development of specific mandrels for creating beveled edges and a smooth inner ring is suggested. This may be accomplished with a Dremel and sanding table or common industrial techniques. In order to improve sintered density further it may be necessary to study the proteins that exist on the cell wall. Further work in understanding the proteins that extend from the cell wall is also essential.

Consideration also needs to be taken for the orientation of the bacteria. Due to the large size, the bacteria may pose as potential voids during sintering. As a future exercise it may be possible to create just the cell wall of the bacteria, neglecting the tip, filament and hook portions of the bacteria.

Summarized future work:

- Development of rings, cylinders and other unusual geometries
- Development of better molds that include easier sample removal
- Specific mandrels
- Bacteria cell wall study and production of the minimal necessary structure for ice templating
- Investigate antifreeze proteins (AFP) which are small enough so that they bind to ice and inhibit further growth without acting as a nucleator

REFERENCES

1. L. Wang, and F. Aldinger, "Near-Net Shape Forming of Advanced Ceramics," *Adv. Eng. Mater.,* **2** [3] 110-3, 2000.
2. S. W. Sofie, "Freeze Forming of Alumina in Aqueous and Non-aqueous Suspension"; M.S. Thesis. University of Washington, WA, 1999.
3. L. R. Maki, E. L. Galyan, M. M. Chang-Chien, and D. R. Caldwell, "Ice Nucleation Induced by Pseudomonas Syringae," *Appl. Microbiol*., **28** 456-9 (1974).
4. D. Clause, "Ice Crystallization Induced by Silver Iodide and Bacteria in Microsize Droplets Dispersed within Emulsions," *Pure Appl. Chem*., **63** [10] 1491-4 (1991).
5. Lockheed Martin, NAVY-I Powder Raw Data. Lockheed Martin, Syracuse, NY, 2013.
6. W. Zhongqin, "Bacterial Low Temperature Survival, Ice Nucleation Proteins and Ice-associating Polymers," Ph.D. Thesis. Queen's University, Kingston, Canada, 2010.
7. B. J. Murray and A. K. Bertram. "Formation and Stability of Cubic Ice in Water Droplets." *Phys. Chem. Chem. Phys.* **8** [1] 186-92 (2006).
8. "Phase Diagram" (2013) Wikipedia, Wikimedia Foundation. Accessed on: September 2013. Available at <http://en.wikipedia.org/wiki/Ice>
9. M. Fernandez-Serra, "The Structure and Entropy of Ice. PHY 313 - Mystery of Matter: Physics of Water" (2011) Stonybrook Univerisity. Accessed on: September 2013. Available at <http://mini.physics.sunysb.edu/~marivi/TEACHING-OLD/PHY313/doku.php?id=lectures:4>
10. D. C. Palmer, CrystalMaker 9 [Computer Program]. CrystalMaker Software Limited Oxfordshire, UK, 2013.
11. T. Fukasawa, "Pore Structure of Porous Ceramics Synthesized from Waterbased Slurry by Freeze-dry Process," *J. Mater. Sci.* **36**, 2523-7 (2001)
12. E. Munch, "Architectural Control of Freeze-Cast Ceramics through Additives and Templating," *J. Am. Ceram. Soc.* **92** [7] 1534-9 (2009).

13. G. J. Morris, “Rapidly Cooled Horse Spermatozoa: Loss of Viability Is Due to Osmotic Imbalance during Thawing, Not Intracellular Ice Formation,” Theriogenology, **68** [39] 804-12 (2007).
14. S. Everts, "Bacteria in Clouds" (2008) Science & Technology. Accessed on: April 2008. Available at <www.CEN-ONLINE.org>
15. “*Icemax: Pseudomonas Syringae*” (2012) Johnson Controls. Accessed on: April 2013. Available at <http://www.fcm.ca/Documents/presentations/2012/webinars/City_of_Saskatoon%20_Two_Examples_Reducing_GHGs_EN.pdf>
16. J. L. Slonczewski, "Pseudomonas Syringae" (2013) BIOL 375 Virology. Kenyon College. Lecture. Accessed on: March 2012. Available at <https://microbewiki.kenyon.edu/index.php/Virulence_of_Pseudomonas_savastanoi>
17. S. E. Lindow, E. Lahue, A. G. Govindarajan, N. J. Panopoulos, and D. Gies, "Localization of Ice Nucleation Activity and the IceC Gene in Pseudomonas Syringae and Escherichia Coli," *Mol. Plant-Microbe Interact.*, **2** [56] 262-72 (1989).
18. D. C. Arny, S. E. Lindow, and C. D. Upper, “Frost Sensitivity of Zeamays Increased by Application of Pseudomonas Syringae,” *Nature*, **4** [July 22] 262-82 (1976).
19. T. Kaneda “Seasonal Population Changes and Characterization of Ice Nucleating Bacteria in Farm Fields of Central Alberta,” *Appl. Environ. Microbiol*., **52,** 173-8 (1986).
20. H. K. Kim, C. Orser, S. E. Lindow and D. C. Sands, “Xanthomonas Campestris pv. Translucens Strains Active in Ice Nucleation,” *Plant Disease*, **71,** 994-7 (1987).
21. S. J. Kim and J. H. Yim, “Cryoprotective properties of Exopolysaccharide (P-21653) Produced by the Antarctic Bacterium, Pseudoalteromonas Arctica,” *J. Microbiol.,* **45**, 510-4 (2007).
22. S. E Lindow, D. C. Arny, and C. D. Upper, “Distribution of Ice Nucleationactive Bacteria on Plants in Nature,” *Appl. Environ. Microbiol*., **36** [6] 831-8 (1978).

23. S. E Lindow, D. C. Arny, C. D. Upper, “Bacterial Ice Nucleation: A Factor in Frost Injury to Plants,” *Plant Physiol.,* **70** [4] 1084-9 (1982).
24. S. E. Lindow, S. S Hirano, W. R. Barchet, D. C. Arny, C. D. Upper, “Relationship between Ice Nucleation Frequency of Bacteria and Frost Injury,” *Plant Physiol.,* **70** [4] 1090-3 (1982).
25. S. E. Lindow, “Competitive Exclusion of Epiphytic Bacteria by Ice Pseudomonas Syringae Mutants,” *Appl. Environ. Microbiol*., **53** [10] 2520-7 (1987).
26. S. E. Lindow, N. J. Panopoulos and B. L. McFarland, “Genetic Engineering of Bacteria from Managed and Natural Habitats,” *Science*, **244** [(4910] 1300-7 (1989).
27. L. R. Maki, E. L. Galyan, M. M. Chang-Chien, and D. R. Caldwell, “Ice Nucleation Induced by Pseudomonas Syringae,” *Appl. Microbiol*., [3] **28** 456-9 (1974).
28. D. Newton and A. C. Hayward, “Ice Nucleation Activity of Some Reference Cultures of Pseudomonas Syringae and Field Isolates of Bacteria from Wheat and Barley in Queensland,” *Australas. Plant Pathol*., **15** [4] 71-3 (1986).
29. H. Obata, N. Muryoi, H. Kawahara, K. Yamade and J. Nishikawa, “Identification of a Novel Ice-Nucleating Bacterium of Antarctic Origin and Its Ice Nucleation Properties,” *Cryobiology,* **38** [2] 131-9 (1999).
30. V. Al’tberg, O tsentrakh ili iadrakh kristaalizatsii vody. Meter. I Gidrol.; pp. 3-12. 1938. Translation: “On Centers or Nuclei of Water Crystallization” Cold Regions Engineering Laboratory, Defense Technical Information Center TL 294, 1972. Available at <http://www.dtic.mil/dtic/tr/fulltext/u2/741054.pdf>
31. A. K. Varshneya, Fundamentals of Inorganic Glasses, 2nd ed.; pp. 3-7. Academic Press, Boston, MA, 2006.
32. “Icemax FAQ” (2013) Milwaukee, Johnson Controls. Accessed in: March 2013. Available at <https://www.beckerarena.com/UserFiles/File/Icemax%20Initial%20FAQ.pdf>

33. "Type Three Secretion System." Wikipedia, Wikimedia Foundation. Accessed on: April 2013. Available at <http://en.wikipedia.org/wiki/Type_three_secretion_system>
34. "Encyclopedia of Surface and Colloid Science" (2006) Materials Chemistry; pp. 4498-4508. Taylor & Francis. Accessed on: October 2012. Available at <http://books.google.com/books/about/Encyclopedia_of_Surface_and_Colloid_Scie.html?id=rlcLQmcTADEC>
35. "Density of Ice and Water as a Function of Temperature." (2013) Wikimedia Commons. Accessed on: April 2012. Available at <http://en.wikipedia.org/wiki/Properties_of_water>
36. R. J. Cava. "Perovskite Structure and Derivatives." Cava Lab: Perovskites. Accessed on: October 1, 2013. Available at <http://www.princeton.edu/~cavalab/tutorials/public/structures/perovskites.html>
37. A. Ballato, "Piezoelectricity: Old Effect, New Thrusts," *IEEE Trans. Ultrason., Ferroelectr., Freq. Control*, **42** [5] 916-26 (1995)
38. Interface Engineering Lab. "Functional Oxide Materials. Department of Chemical Engineering." Northeastern University. Accessed on: November 2013. Available at <http://www1.coe.neu.edu/~kziemer/>
39. "Heckmann and Thurston Diagrams." Flickr. Yahoo!, Accessed on: August 2013. Available at < https://www.flickr.com/photos/36402008@N06/3491794115/?rb=1>
40. "Mil-Std-1376b, Military Standard: Piezoelectric Ceramic Material and Measurements Guidelines for Sonar Transducers" (1995) [No S/S Document] Department of Defense. Accessed on February 2013. Available at < http://www.everyspec.com/MIL-STD/MIL-STD-1300 1399/MIL_STD_1376B_666/>
41. Johnson Controls. "Icemax." Johnson and Johnson, (2011), Accessed on January 2014. Available at <http://www.johnsoncontrols.com.sa/content/sa/en/products/building_efficiency/aftermarket-services-energy-solutions/building/ice_rinks/ice_arena.html>
42. CambridgeSoft Corp, ChemDraw 10.0 Std. Cambridge, MA, 2006.

43. G Fahy and B Wowk, “Prevention of Ice Nucleation by Polyglycerol,” U.S. Pat. 20020063235 A1, September 2003.
44. "Home of the Thermapen." ThermoWorks.com. Accessed on June 2012. Available at <http://www.thermoworks.com/>
45. R. Jenkins and R. L. Snyder, *Introduction to X-ray Powder Diffractometry*. Wiley, New Work, 1996.
46. G. Elert, *The Physics Factbook*. (1992) Midwood High School, Brooklyn, NY. Accessed on: January 2014. Available at <http://hypertextbook.com/facts/2000/AlexDallas.shtml>
47. Morgan Electro Ceramics, “Piezoelectric Ceramics,” MorganElectroCeramics, Bedford, OH, 2007.